A mesoscopic analysis of cavities in two components silicone adhesive with cylindrical butt joint specimens

R. Seewald[1], M.A. Schnittcher[1], F. Pauly[2], S. Rath[2], B. Schaaf[3], L. Lamm[4], A. Schiebahn[1], T. Brepols[4], S. Reese[4], M. Feldmann[3], U. Reisgen[1]

[1]Welding and Joining Institute – RWTH Aachen University, Pontstr. 49, 52062 Aachen, Germany
[2]Forschungszentrum Jülich GmbH, Wilhelm-Johnen-Straße, 52428 Jülich, Germany
[3]Institute of Steel Construction – RWTH Aachen University, Mies-van-der-Rohe-Str. 1 52074, Aachen, Germany
[4]Institute of Applied Mechanics – RWTH Aachen University, Mies-van-der-Rohe-Str. 1 52074, Aachen, Germany

Corresponding author: Robert Seewald, seewald@isf.rwth-aachen.de

Abstract

In the construction industry, silicone adhesives were firstly used as sealant because of their elasticity and resistance towards environmental exposition. Nowadays, modern façades need to fulfil thermal efficiency, while keeping transparent design. Structural glazing façades satisfy these requirements due to silicone adhesives. However, because of the complex nonlinear material behaviour of silicone adhesives, only a conservative dimensioning with linear material law using high safety factors is proposed in the European guideline ETAG 002.

This investigation aims to quantify cavities in cylindrical butt-bonded specimens on a mesoscopic scale in two-component silicone adhesive for layers at minimum ETAG 002 requirement (4 mm). As hydrostatic tensile stress accounts for cavities,

the necking transversal to the load has been monitored with digital image processing during tensile tests. In the developed in-situ tensile aperture cavities have been quantified with an X-ray micro-computed tomography (Micro-CT) on a mesoscopic scale at defined strain. With scanning electron microscopy (SEM) footprints of cavities on the fracture surface can be observed. As main conclusion cavities have been visualised in-situ under tensile load and quantified to volumes ranging from 0.0055 mm^3 to 0.194 mm^3.

Keywords: silicone adhesive, cavities, structural glazing, material behaviour

Introduction

Typical Structural sealant glazing (SSG) façades consist of a glazing bonded to a support frame by silicone adhesive. The bonded element is then connected to the façade substructure. Wind loads on the glazing are carried by the adhesive. If required by the building authorities redundant fixing systems are used to bear the deadload of the glazing, which, however, is also possible without any problems by the adhesive, or to prevent falling of the glazing in case of adhesive failure. The schematic design of an SSG construction is shown in Fig. 1. Started in the 1960s in the USA [1], this construction technology is now used worldwide for façades with high transparency requirements, e.g. the train station Hungerburg in Innsbruck, Austria (Fig. 2).

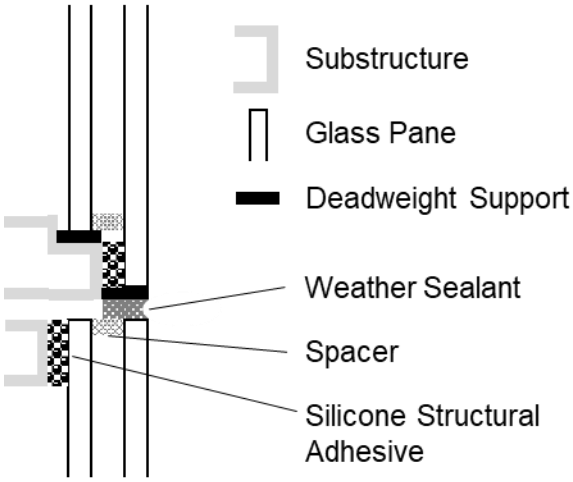

Fig. 1 : Structural Glazing façades

Fig. 2 : Structural Glazing - Train Station Hungerburg, Innsbruck, Austria

The European guideline ETAG 002 [1] allows the dimensioning of silicone adhesive layers based on a linear material behaviour. As silicone adhesive shows a nonlinear (hyperelastic) material behaviour and the damage behaviour of the silicone adhesive is unknown the ETAG 002 [1] applies high safety factors. A defined damage behaviour would result in a more realistic design, higher transparency, less material use and a more knowledge driven calculation and application of the adhesive layer.

Cavitation of soft hyperelastic adhesives

Due to the slope break in rubber-like materials, cavities were firstly observed and associated to the failure of the bulk material by Gent and Lindley [3]. Especially under high hydrostatic tensile stresses cavities can be observed. Therefore, cylindrical butt-bonded and thin layered specimens are favourable to achieve a hydrostatic tensile stress in the bulk material. Within experimental investigation

Hocine et al. [4] showed the influence of different thicknesses on occurrence of cavities within the adhesive. It was also possible to show the change in bulk volume. Hamdi et al. [5] investigated different limiting criteria for the occurrence of cavities and propose the hydrostatic pressure and the global deformation. Drass and et al. [6] investigated cavities with a camera through a glass pane in a pancake test of a thin layered transparent one-component silicone adhesive. The cavitation effect and the failure patterns have yet only been investigated on a macroscopic level, especially for two-component silicone adhesives widely used for structural glazing applications.

The failure of rubber-like materials is often associated with the internal growth of voids or cavities. The initiation of cavities was first documented by Busse [7] on cylindrical thin-layer adhesive joints. These so-called "pancake" specimens were exposed to a tensile load up to complete failure and cavities were found in the centre of the specimens on the fracture surface. In a similar investigation by Gent & Lindley [3], the formation of cavities was justified with a triaxial (hydrostatic) stress state and the slope break in the stress-strain diagram was correlated with the initiation of cavities. In [9] and [10] Drass et al. developed a pseudo cavitation model based on [8] for adhesive point fixings in glass construction for transparent structural silicone adhesives (TSSA) adhesives. The aim of the current research is to characterise the cavitation in butt-joint specimens under hydrostatic tensile stress for typical silicone adhesives used in SSG applications.

Materials & Methods

For the characterisation of cavities in silicone adhesive, three different methods were used according to the damage evolution. Micro X-Ray CT was utilised to visualise and quantify the cavitation effect prior to damage. The necking behaviour was measured with video-extensometry and digital image processing (DIP) during the damage evolution and after full fracture the macroscopic crack shapes were documented with a confocal microscope. Finally, the fracture surface was analysed with scanning electron microscopy (SEM) on a microscopic level.

For all analyses the same cylindrical butt joint specimens and the two-component silicone adhesive Ködiglaze S, HB Fuller / Kömmerling Chemische Fabrik GmbH, Pirmasens, Germany, is used. The specimen are prepared according to the German standard DIN EN 15870 [11]. The cylindrical adherends are made of structural steel (S235 JR) with a diameter of 20 mm and a length of 60 mm. The butt surface has been prepared using the abrasive fleece 3M Scotch-Brite 220, 3M Deutschland GmbH, Neuss. Due to the excellent adhesive properties of silicone adhesive compared to its cohesive strength, no further surface preparation is required to achieve a cohesive fracture of the bonded specimen. The adhesive is applied from a two-component cartridge (490 ml) with a static mixer. The adhesive layer thicknesses of 2, 4 and 6 mm have been realised by using appropriate spacers in the production fixture. Radially escaping adhesive is removed with a razor blade after 24 hours to obtain a cylindrical adhesive layer.

For the tensile testing of the specimens, the universal testing machine RetroLine Z010 from Zwick GmbH & Co. KG, Ulm, is used (Fig. 3 (a)). The machine frame of the universal testing machine is designed for a maximum load of F_{max} = 10 kN. The tensile tests carried out within this work are all below 1 kN, whereby an influence of the machine stiffness on the test results can be neglected. The specimen is suspended with bolts in a gimbal on the testing machine. The external tensile load of the testing machine (Fig. 3 (b)) exhibits hydrostatic tensile stresses in the adhesive due to the transversal contraction (Fig. 3 (c)).

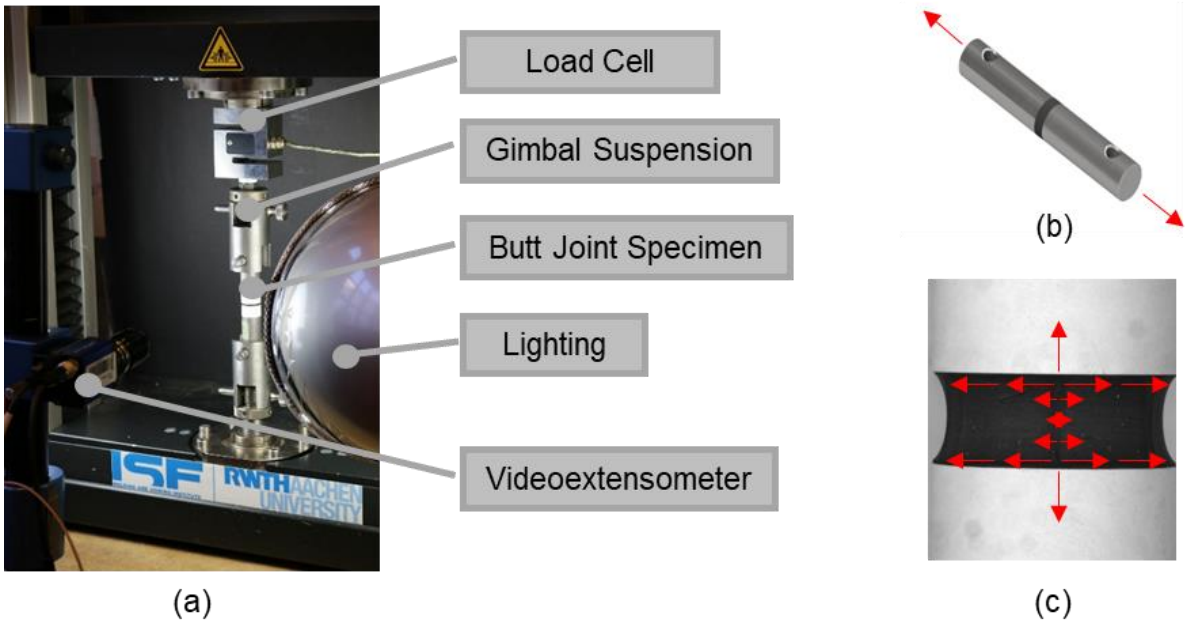

Fig. 3 : (a) Tensile testing setup, (b) Cylindrical butt joint specimens, (c) Theoretical hydrostatic tensile stresses in silicone adhesive

All specimens were cured for 7 days at room temperature (23 °C) with a relative humidity of 50 % and loaded with a true strain rate of 10 %/min. (relative to the distance of the adherends) to account for the high strains of silicone prior to failure.

1. Prior to damage – Micro X-Ray Computertomography

In total three specimens are analysed with X-Ray Computertomography (Fig. 4 (a)). The thickness of the adhesive was set to 4 mm to account for the minimal ETAG 002 thickness while maximising hydrostatic tensile stresses within the adhesive. Two specimens are preconditioned with 10 cycles at the global strains of $\varepsilon = [25, 100]$ % on the tensile testing machine, one specimen remains unloaded. The X-Ray CT scans of the silicone adhesive were then performed with the in situ testing machine (Fig. 4 (b)) for each specimen (unloaded and loaded) at $\varepsilon = 25$ %, which was measured with a calliper gauge through an inlet in the in situ testing machine.

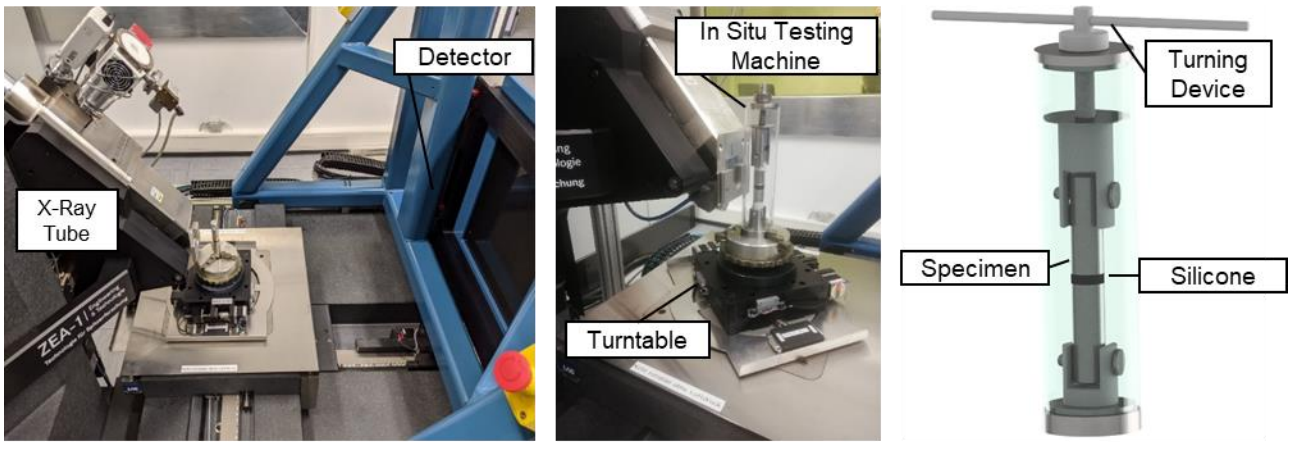

Fig. 4: (a) Micro X-Ray CT at Forschungszentrum Jülich, Germany, (b) In Situ Testing Machine fixed on a turntable, (c) In Situ Testing Machine for cylindrical butt joint specimens for silicone adhesive

The voxel resolution of the X-Ray CT scans is set to 0.0123 mm and saved in DICOM format. The DICOM Data is computed using Digital Image Processing & Computer Vision Toolbox of Matlab. A visualisation of cavities is performed using volume rendering for each scan equally. For the segmentation and quantification of cavities the active contour algorithm of Chan-Vese was utilised. The algorithm iteratively fits a locally defined 3D mask created from XY and XZ slices to the given volume. The result is a 3D volume of a cavity, which is labelled in the original silicone adhesive volume for verification purposes. The volume of a cavity is calculated by the total number of voxels and the known resolution of the CT scan.

2. Damage Evolution – Videoextensometry

The macroscopic analysis includes adhesive thicknesses of [2, 4, 6] mm with a series of each five specimens. The adhesive thicknesses account for the minimal allowed ETAG 002 thickness of 4 mm, the minimal allowed thickness in in some EU member states of 6 mm (recommended by ETAG 002) and a thickness of 2 mm below the current allowed thickness. During the tensile test, the specimens were monitored with a videoextensometer, which measured the elongation of the adhesive. As the transversal necking is in a different focus area compared to the elongation, a direct monitoring of the necking with the videoextensometer showed inaccurate results. Instead images were recorded by the camera of the videoextensometer, which allowed a calculation of the necking in a self-developed program in Matlab. The pictures were recorded with a frequency of 1 Hz to limit the amount of data. The images are read in a self-developed Matlab program (Fig. 5),

which binarises the images and calculates the change in diameter in the centre of the adhesive as well as the strain according to the measured elongation.

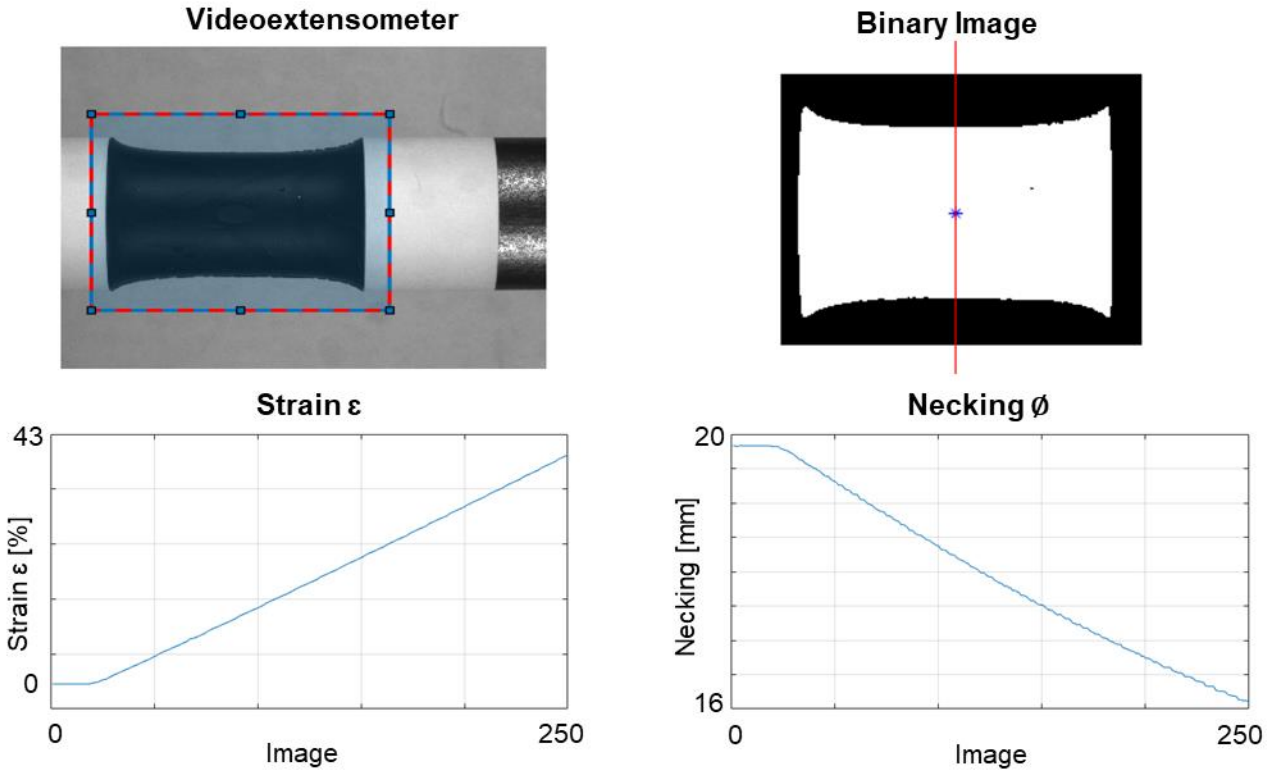

Fig. 5 : Matlab Program – Necking of Silicone Adhesive

A 6th degree polynomial is used to plot the strain necking curve of 1 Hz. During the tensile test the force and strain are recorded with a frequency of 20 Hz. In order to calculate the true stress for the silicone adhesive, the necking is upsampled to 20 Hz with the 6th degree polynomial and the recorded strain value of 20 Hz.

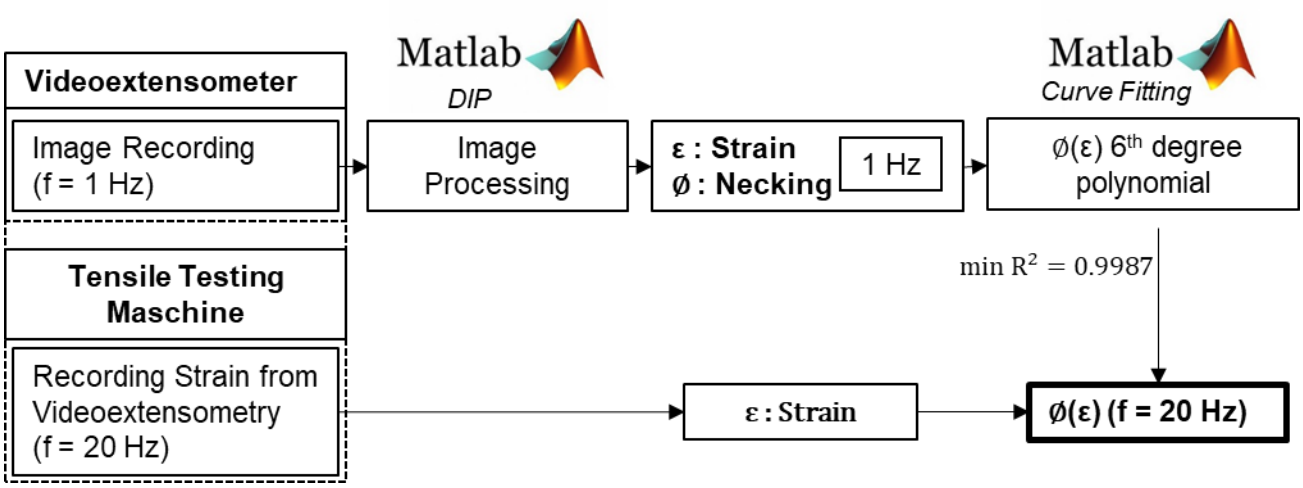

Fig. 6 : Process to upsample necking data

3. Post Damage – Scanning Electron Microscopy

For the analysis of cavities on a microscopic level of the fracture surface a scanning electron microscope (SEM) was utilised. A pair of unloaded cylindrical butt bonded specimens and a pair of fractured specimens with a thickness of 4 mm was analysed at four predefined locations according to Fig. 7. The two locations at the interface between adhesive and adherend account for the highest hydrostatic stresses in the adhesive, while the central location (M_a^G) experiences the highest transverse contraction and the edge location (R_a^G) a high strain. To investigate those areas, the specimens have been cooled down in liquid nitrogen (LN_2) for separating adhesive and adherend with a sharp cutting blade in order to obtain a clean cut without further damage infliction [6]. The location (M_a^C) is located in the centre of the adhesive and the location (R_a^C) at the edge accounts for the maximum necking of the adhesive. The analysis takes place respectively on the accessible surface of the adhesive.

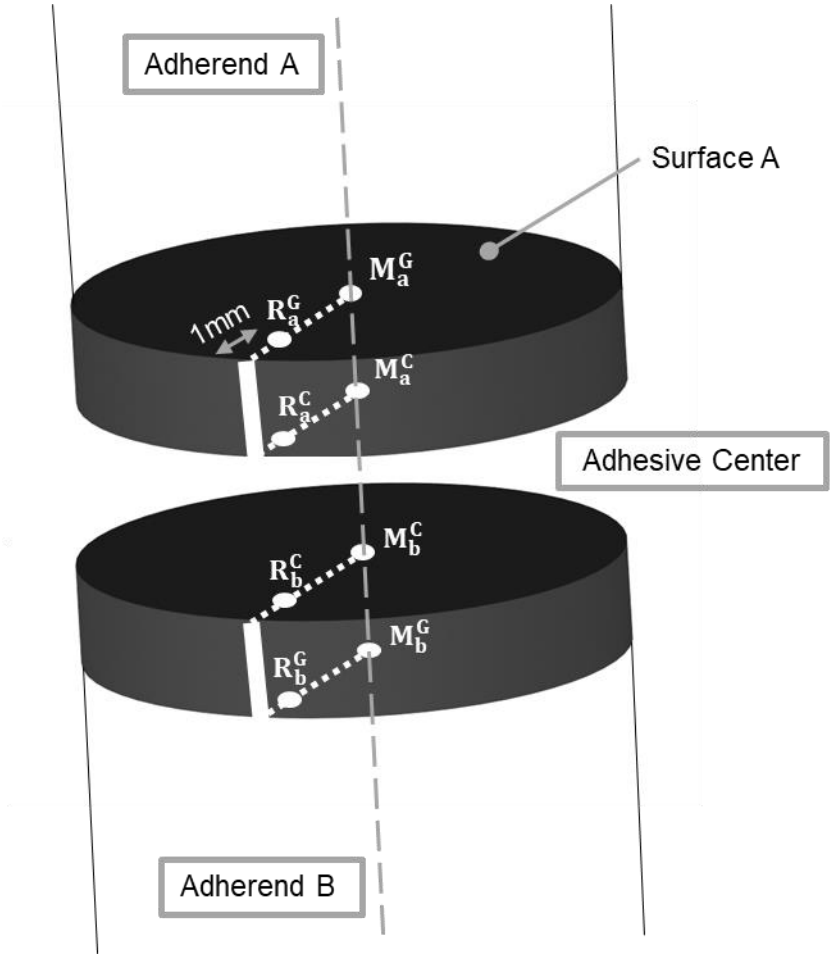

Fig. 7 : Analysed Locations with SEM

To observe cavities in the transition zone between the adhesive and the adherend with SEM, it was necessary to separate the silicone from the steel substrate. According to the procedure of Drass [6] all specimens were put in liquid nitrogen for half hour and cut off with a knife from the adhesive in order to minimize further damage effects while cutting due to the highly rigid material behaviour under cryogenic conditions.

Results

In the following, the results of each method to analyse the cavitation in silicone adhesive are presented.

1. Prior to damage – Micro X-Ray Computertomography

As first method, the results of the Micro X-Ray CT are discussed, since they describe the specimen condition before a complete failure or crack. In the following three different preconditioned butt joint specimens at two different in situ strain levels are shown. The volume of cavities in the silicone adhesive is visualised (Fig. 8). Especially for the unloaded specimen at $\varepsilon = 25\%$ in situ strain, some major voids appear. The major voids arise from a production defect, as the void appears also slightly at $\varepsilon = 0\ \%$ in situ strain. An initiation of cavities was observed in the centre of the adhesive layer.

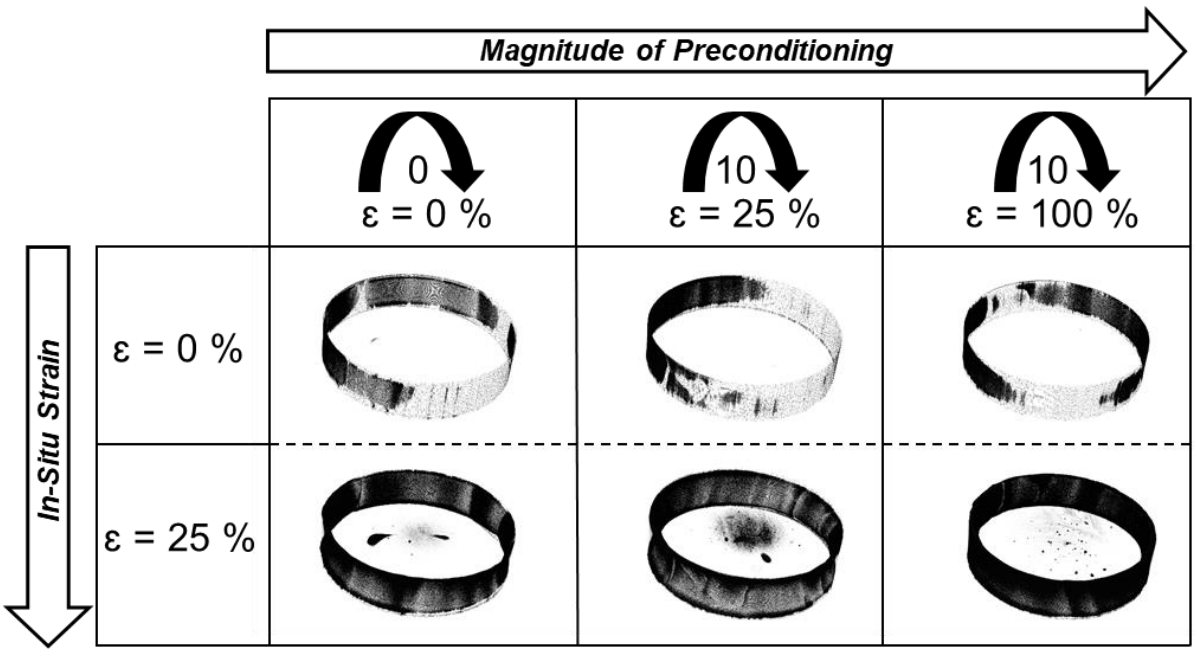

Fig. 8 : Visualisation of cavities in silicone adhesive for different magnitudes of preconditioning

In the centre of all specimens at ε = 25 %, noise or cavities, smaller than the resolution of the CT, are appearing. The segmentation of cavities is challenging, as the gray values of the noise is similar to visible cavities. As an example, the most cavitated specimen with a preconditioning at ε = 100 % at in-situ strain of ε = 25 % was further analysed with respect to the volume of the cavities. Due to a high computational effort and no available automation algorithm, the volume of

three different sized cavities was calculated and visualised. All other visible cavities were assigned to the corresponding volume according to their size (Fig. 9).

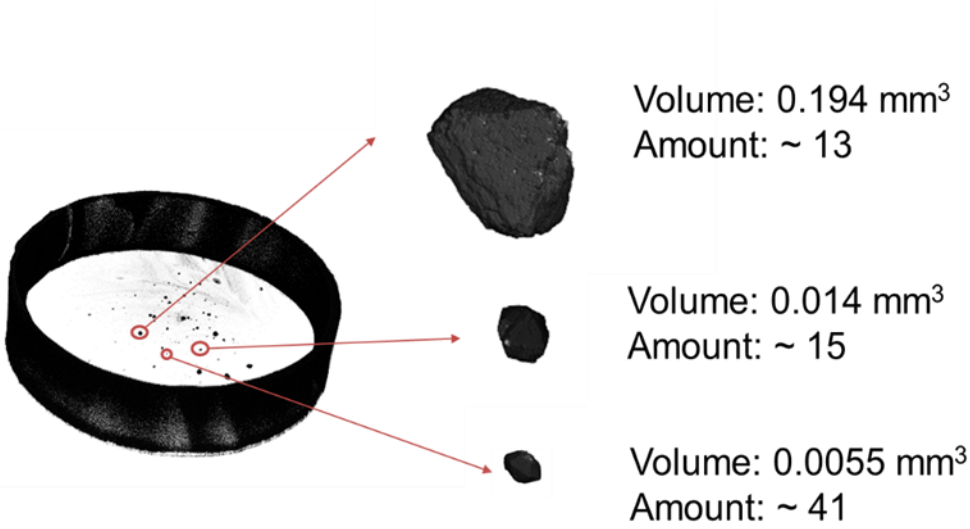

Fig. 9: Quantification of of cavities – preconditioning of ε = 100 % at in situ ε = 25 %

In this way the total cavitation volume was estimated to 2.9575 mm^3. Based on the initial adhesive volume of 1256.63 mm^3 it results in a volume loss of 0.2354 %. On the same specimen with no in-situ strain (ε = 0 %) the visualisation does not show any detectable cavity.

2. Damage Evolution – Videoextensometry

In Fig. 10 the necking behaviour of butt joint specimen at different thicknesses is presented. The curves represent the mean value for the series of specimens and the shaded area represents the standard deviation. For all thicknesses, the necking behaviour is nonlinear and rapidly increasing at low strains, while being almost linear at higher strains. It can be observed that the necking increases with a higher

adhesive thickness. Since a higher adhesive thickness corresponds to a lower transverse contraction in the centre of the adhesive layer, more deformation is possible. Moreover, the magnitude of necking does not linearly correspond with the adhesive thickness. The difference of necking between 2 mm specimens and 4 mm specimens is way higher compared to the necking between 4 mm specimens and 6 mm specimens.

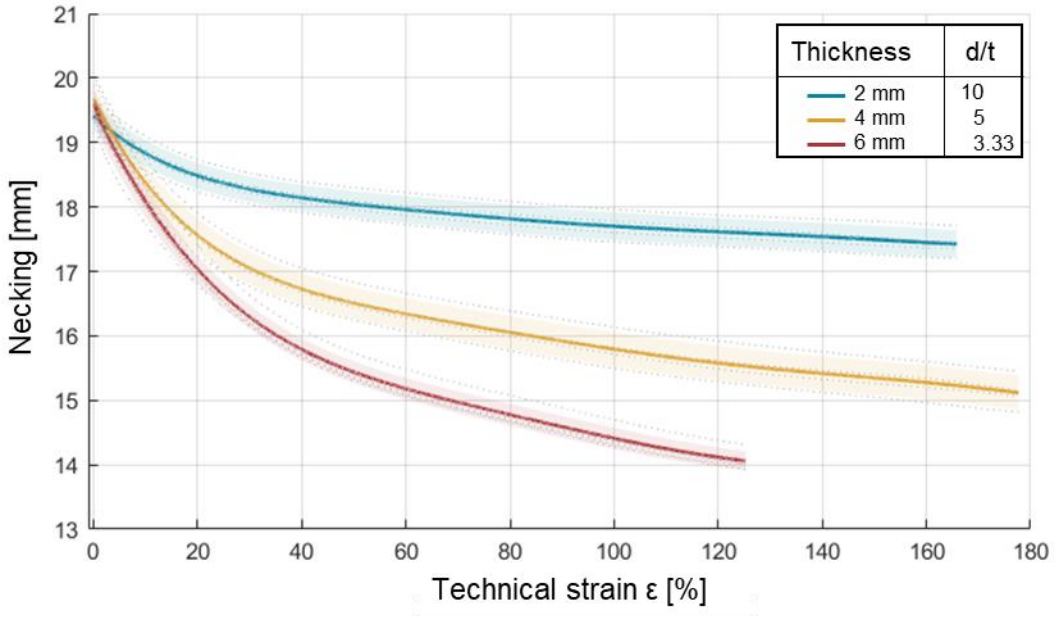

Fig. 10: Necking of butt joint silicone adhesive specimens for thicknesses of 2, 4 and 6 mm

Lower necking is an indicator for a higher transversal contraction and, therefore, higher hydrostatic stresses. As silicone adhesive is a high elastic material the technical stresses do not match the true stresses anymore. With the known necking behaviour, the true stresses in the centre of the adhesive can be calculated. In Fig. 11 the technical stresses are compared to the true stresses. The mean curves with the respective shaded standard deviation are displayed for each thickness. The specimens with a thickness of 2 mm exhibit the highest stiffness compared to

4 mm and 6 mm. As expected, the true stress for all thicknesses is higher compared to the technical stress. Moreover, for low strains up to 25 % a nonlinear behaviour can be observed.

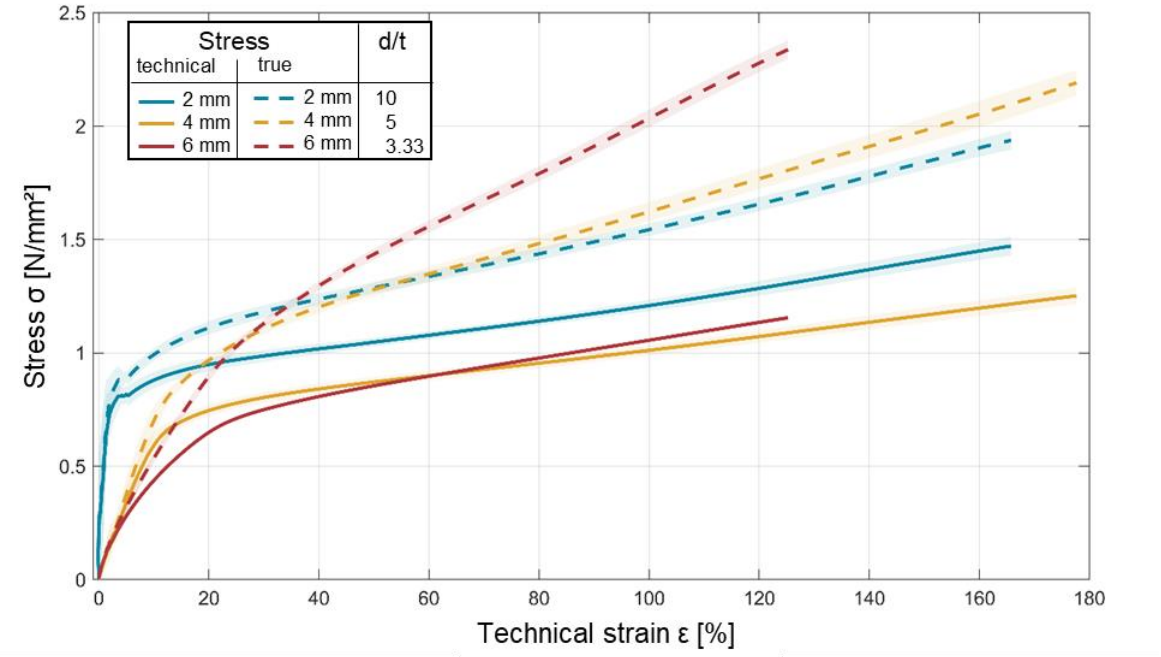

Fig. 11 : Technical/True stress for silicone adhesive at thicknesses of 2, 4 and 6 mm

After failure of the specimens the crack shapes were photographed and scanned with a confocal microscope (Fig. 12). The crack shapes show more peaks for lower thicknesses, which can be related to higher hydrostatic stress fractions. The thicker the adhesive layer the fewer peaks occur in the fracture pattern and the more a simple tensile stress dominates.

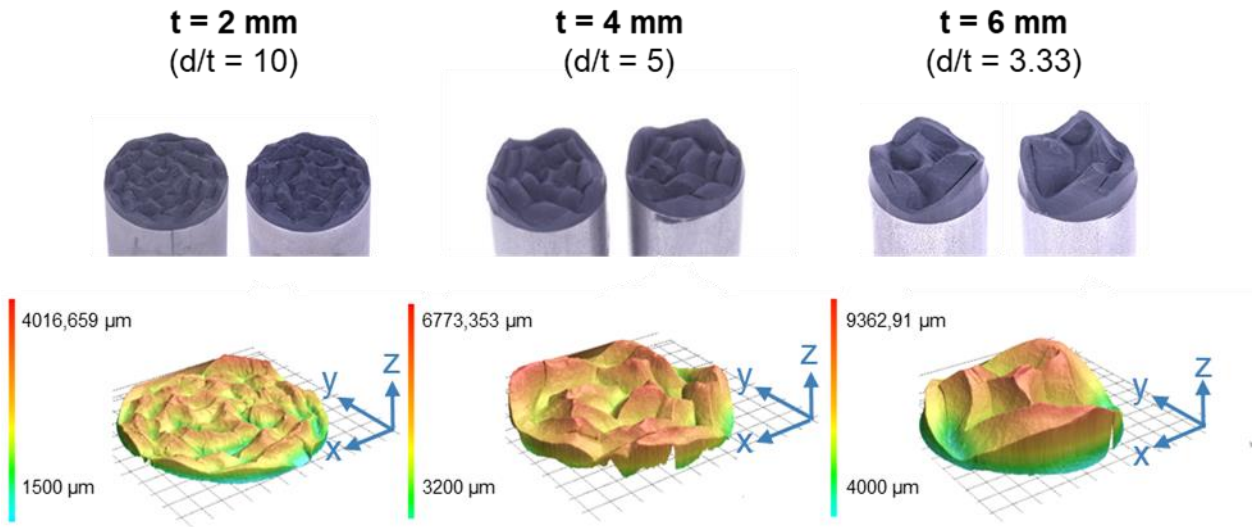

Fig. 12 : Fracture surface for silicone adhesive at thicknesses of t = [2, 4, 6] mm

3. Post Damage – Scanning Electron Microscopy

As third analysis method, the fracture surfaces of the specimens after complete failure are investigated by scanning electron microscopy. Images at the four investigated locations with the SEM are shown at a magnification of factor 1000 in Fig. 13.

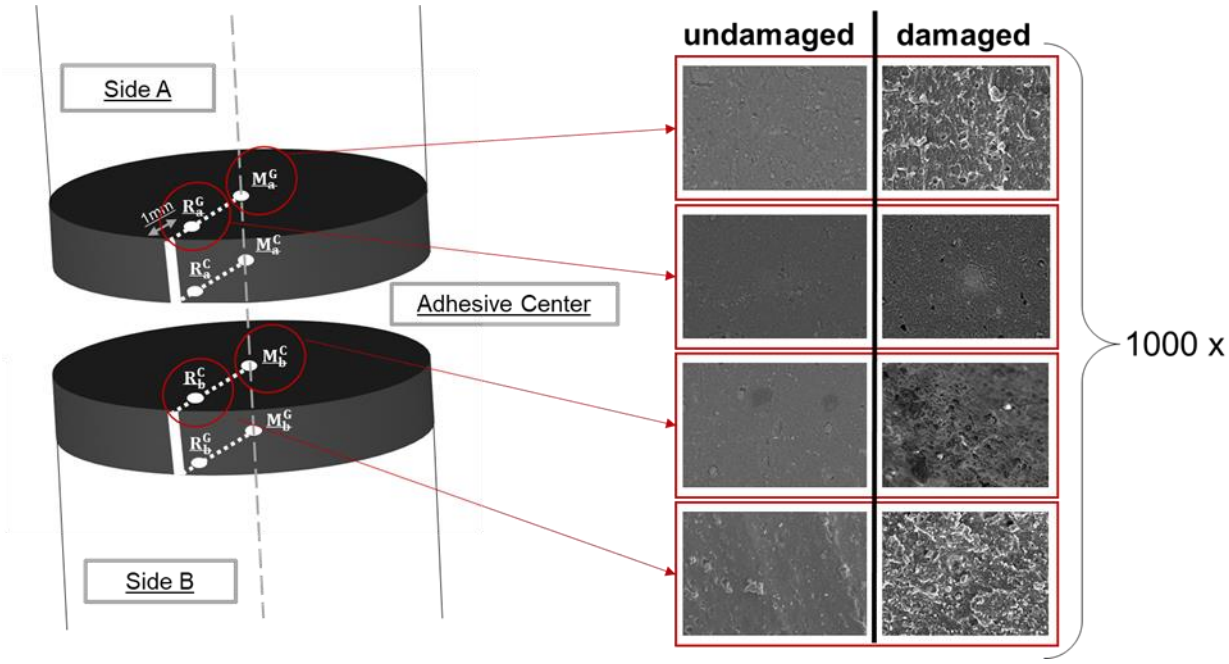

Fig. 13 : SEM images of undamaged and damaged surface

As can be seen in the pictures, the surface of the loaded and unloaded specimens show a significant different texture. While the undamaged specimen shows an almost uniform and flat surface, the damaged one has a significantly rougher and more porous surface. For further investigation, the location in the centre of the adhesive (M^C) is shown in higher magnification in Fig. 14. On the unloaded surface one major cavity can be observed, while the completely damaged surface is highly

porous with cavities ranging from 3 to 20 µm. On each surface one cavity is measured at a magnification of 5000.

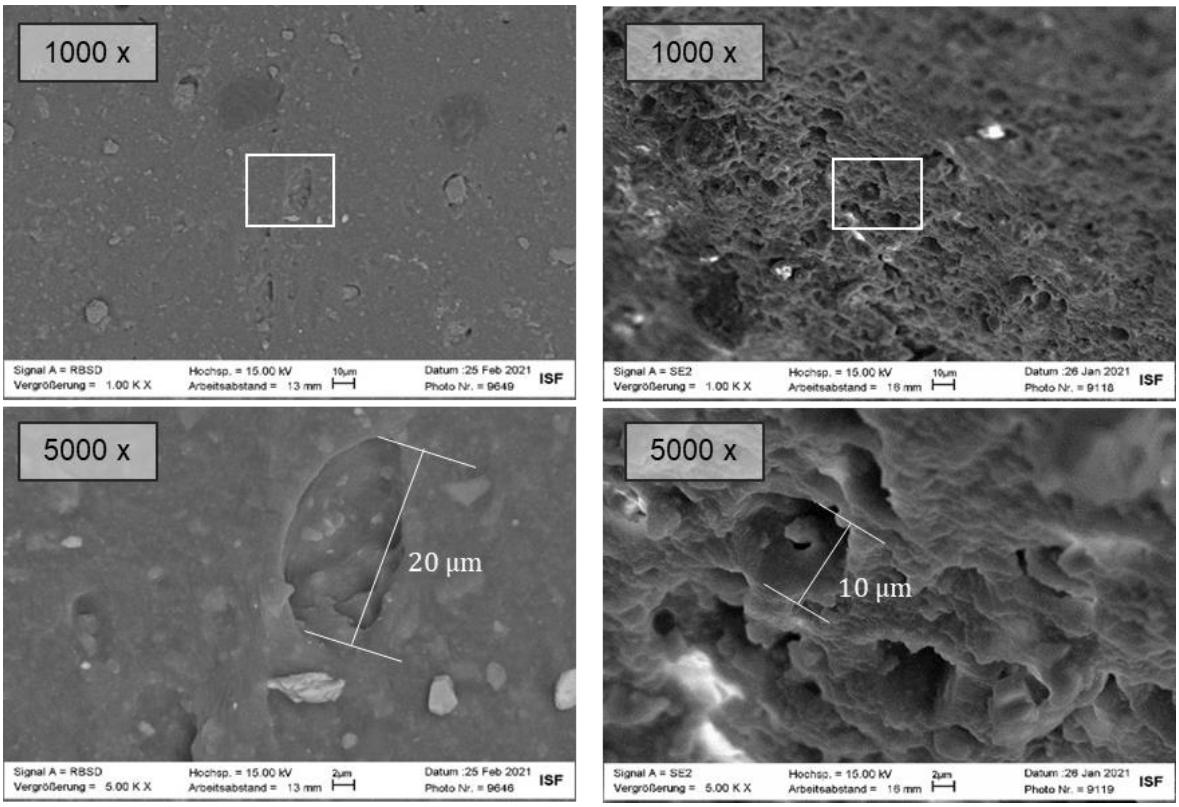

Fig. 14: Silicone surface under undamaged (left) and damaged (right) condition, magnification of factor 1000 and factor 5000

Conclusion

Cavities appear especially in the centre of the adhesive and can be visualized in different analyses. The interfaces of the adhesive and adherend have the highest fractions of hydrostatic stress, but do not show a higher cavitation. The failure of silicone adhesive starts at maximum transversal strain constraint and respectively hydrostatic stress from outside to inside. Higher fractions of hydrostatic stress have an effect of the topography of the fracture surface. The interaction of the stress states in the centre and the maximum of hydrostatic stress fractions at the interface

is suspected to cause a sawtooth like crack shape. In this interaction cavities are suspected to build damage initiation. Cavities can be visualised from CT Data with volume rendering and quantified in volume, but further work on the automated segmentation is needed to gain more precise information about the volume loss prior to failure of the adhesive.

Acknowledgement

These presented results were developed within the framework of the research project “*Versagensprognose hyperelastischer Klebstoffe*”, IGF-No. 21348 N. The project was funded by the Arbeitsgemeinschaft industrieller Forschungsvereinigungen "Otto von Guericke" e.V. (AiF) from funds of the Federal Ministry of Economic Affairs and Energy (BMWi) based on a decision of the German Bundestag and is supported by DECHEMA Gesellschaft für Chemische Technik und Biotechnologie e. V.

Supported by:

on the basis of a decision
by the German Bundestag

References

[1] ETAG 002, Guideline for European Technical Approval for Structural Sealant Glazing Kits, European Organisation for Technical Approvals, (2012).

[2] J.R. Hilliard, C.J. Parise, C.O. Peterson, Structural Sealant Glazing. Sealant Technology in Glazing Systems, ed. C. Peterson ASTM International, pp. 67-99 (1977)

[3] A. N. Gent and P. B. Lindley, Internal Rupture of Bonded Rubber Cylinders in Tension, Proceedings of the Royal Society of London. Series A, Mathematical and Physical SciencesVol. 249, No. 1257 (1959)

[4] N. Aït Hocine, A. Hamdi et. al., Experimental and finite element investigation of void nucleation in rubber-like materials, International Journal of Solids and Structures 48 (2011) pp. 1248–1254.

[5] A. Hamdi, S. Guessasma, M. Naït Abdelaziz, Fracture of elastomers by cavitation, Materials and Design 53 (2014), pp. 497–503.

[6] M. Drass, J. Schneider and S. Kolling, Novel Volumetric Helmholtz Free Energy Function accounting for Isotropic Cavitation at Finite Strains, Materials & Design Volume 138, (2018)

[7] W. F. Busse, Physics of Rubber as Related to the Automobile. Journal of Applied Physics 9 (1938), 7, S. 438–451.

[8] M. Drass, On cavitation in transparent structural silicone adhesive: TSSA. Glass structures & engineering 3 (2018), 2, pp. 237–256.

[9] M. Drass, P.A. Du Bois, J. Schneider, Pseudo-elastic cavitation model: part I—finite element analyses on thin silicone adhesives in façades, Glass Struct. Eng. (2020) 5:41–65.

[10] M. Drass, P.A. Du Bois, J. Schneider, Pseudo-elastic cavitation model: part II—finite element analyses on thin silicone adhesives in façades, Glass Struct. Eng. (2020) 5:67–82.

[11] DIN EN 15870, Deutsches Inistitut für Normung e.V., Adhesives – Determination of tensile strength of butt joints (ISO 6922:1987 modified), European standard (2009).